Eolian and fluvial sedimentation in the southwestern Sinai Mountains, Egypt: a record of flash floods during the late Pleistocene

Jörg Völkel, Jörg Grunert, Matthias Leopold, Kerstin Hürkamp, Juliane Huber and Andrew Murray

ABSTRACT

Wadis emerging from the southwestern Sinai Mountains (Egypt) westwards to the Gulf of Suez are filled by >40 m thick late Pleistocene sediments, which have been subsequently incised to bedrock after the Last Glacial Maximum (LGM). Sedimentation and erosion resulted from changes in the basin's hydrological conditions caused by climate variations. Sediment characteristics indicate distinct processes ranging from high to low energy flow regimes. Airborne material is important as a sediment source. The fills are associated with alluvial fans at wadi mouths at the mountain fronts. Each alluvial fan is associated and physically correlated with the respective sediment fill in its contributing wadi. The alluvial fans have steep gradients and are only a few kilometers long or wide. The alluvial fans converge as they emerge from the adjacent valleys. According to optically stimulated luminescence dating, the initial sediment has an age of ~45 ka and the sedimentation ends ~19 ka, i.e., happened mainly during marine isotope stage (MIS) 3 and early MIS 2 formation and initial incision sometime during LGM. As the delivery of sediments in such a hyper-arid environment is by extreme floods, this study indicates an interval of intense fluvial activity, probably related to increased frequency of extreme floods in Southern Sinai. This potentially indicates a paleoclimatic change in this hyper-arid environment.

Key words | alluvial fans, flash floods, late Pleistocene climate, MIS 3, Sinai Mountains, wadi fillings

Jörg Völkel (corresponding author)
Matthias Leopold
Juliane Huber
Technische Universität München,
Center of Life and Food Sciences Weihenstephan,
Chair of Geomorphology and Soil Science,
85350 Freising,
Germany
E-mail: *joerg.voelkel@tum.de*

Jörg Grunert
Johannes Gutenberg Universität Mainz,
Institute of Geography,
55099 Mainz,
Germany

Kerstin Hürkamp
Helmholtz Zentrum München,
Institute of Radiation Protection,
85764 Neuherberg,
Germany

Andrew Murray
The Nordic Laboratory of Luminescence Dating,
Risø National Laboratory,
4000 Roskilde,
Denmark

INTRODUCTION

Dryland streams are characterized by relatively long time intervals without flow. Significant fluvial activity in extremely arid regions is associated with infrequently occurring large floods (Baker 1977; Graf 1988; Tooth 2000). The drainage system of the Southern Sinai magmatic–metamorphic massif consists of many dry river beds (wadis), associated with tectonic lineaments. In the western part of Southern Sinai, the canyon-like wadis drain towards the Gulf of Suez (Figure 1). In nearly all the lower reaches of these canyons, thick sedimentary fills of different textures, compositions and origin are exposed. They include eolian deposits that are partially fluvially reworked. All these wadi fills are connected with extensive alluvial fans downstream at the exit of the wadis towards the El Qaa coastal plain (Figure 1). The existence, composition, age, and interpretation of genesis of these alluvial and eolian deposits in the southwestern Sinai wadis have rarely been investigated. Only the fluvially reworked, loess-like sediments of Wadi Feiran were documented by Rögner *et al.* (1999). These authors present thermoluminescence (TL) dating for these fine-grained wadi fills, ranging between 27 and 11 ka. The data fall within the marine isotope stage (MIS) 2 and thus cover the period pre-Last Glacial Maximum (LGM) and deglaciation (Imbrie *et al.* 1984). We use the LGM definition following Mix *et al.* (2001) as the time around 21,000 years ago. Previous investigators interpreted the fine-grained sediments as glacial moraines (Fraas 1867) or lacustrine sediments deposited behind local dams, produced by

doi: 10.2166/nh.2012.172

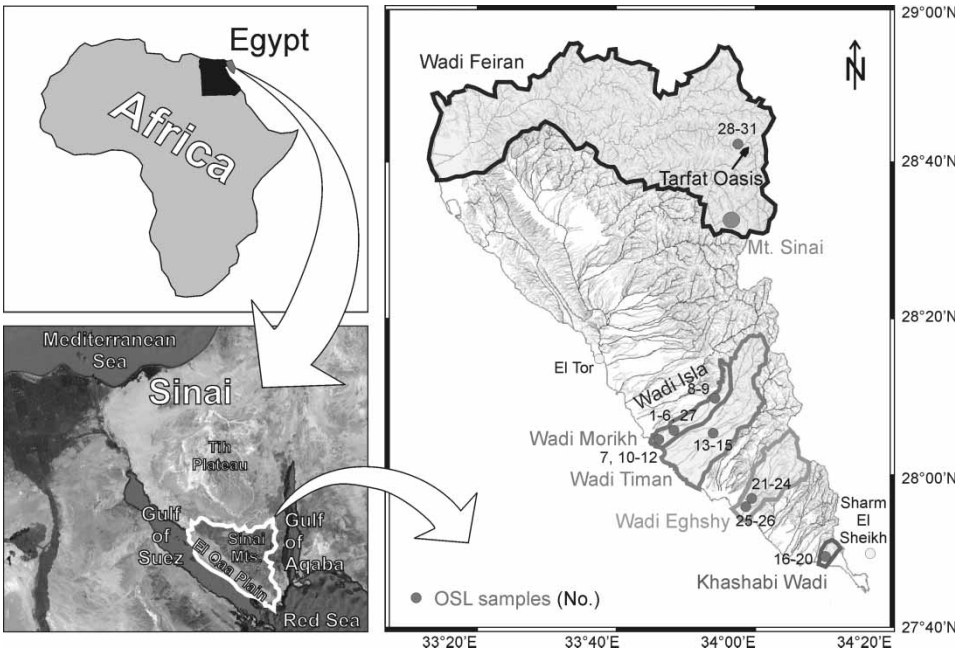

Figure 1 | Watershed map showing the catchments of the five investigated wadis, draining the southwestern Sinai Mountains and opening out into the adjacent El Qaa coastal plain and the Gulf of Suez. Sampling points for OSL age determinations are marked by dots and are numbered according to the sample numbers given in Table 3. (Hydrographic base map modified according to Sherief (2008)). Additionally, points of interest mentioned in the text are marked.

rockfalls or landslides (e.g., Barron 1907; de Martonne 1947; Awad 1951, 1953; Issar & Eckstein 1969; Nir 1970, 1974). Büdel (1954) and Klaer (1962) first interpreted the silts as fluvial terraces. Rögner *et al.* (2004) and also Knabe (2000), Smykatz-Kloss *et al.* (1999/2000, 2000, 2003) concluded that most of the silts were alluvially relocated desert loess after reconsidering their own interpretation of a lacustrine origin (Rögner & Smykatz-Kloss 1998; Smykatz-Kloss *et al.* 1998). Deposition of eolian sediments within fluvial systems is also known from other arid regions (e.g., Leopold *et al.* 2006; Heine & Völkel 2009, 2010, 2011). The sediment source of the Wadi Feiran can be partially traced to outcrops of Miocene marls in the Ataqa anticline of the Gulf of Suez (Bayer *et al.* 1988) according to the occurrence of foraminifera in the loess. During the LGM (MIS 2), the sea-level was 122 m lower than today (Gvirtzman 1994). Thus, an eolian transport of the marls up to the hills and wadi slopes of the southwestern Sinai mountain rim was enabled. The silts were later washed out by rain, transported in a meandering river, and deposited as overbank fines on the narrow plains behind the levees, as crevasse splays or in swampy environments possible in the rare cases of existing natural dams within the river channels. These dams could have been caused by migrating alluvial fans of tributary valleys. The alternation of the valley fills with coarse-grained fluvial material is due to the weathering of bedrock upstream and deposition as point bars in river beds or as alternative layers above the silts when the river changed its bed (Rögner *et al.* 2004).

In this study, the fluvial deposits of five wadis of the southwestern Sinai Mountains are described and dated by optically stimulated luminescence (OSL) techniques. The geochronology of late Pleistocene sedimentation and erosion processes help to determine changes in hydrogeomorphic regimes probably controlled by climatic variations or by minor changes in characteristics of precipitation or wind intensity and persistency, which do not necessarily imply a response to a major climatic change.

REGIONAL SETTING

The study area is in eastern Egypt in the southern part of the Sinai Peninsula, which is framed by the shallow Gulf of Suez (<80 m under sea level) and the deep Gulf of Aqaba (or Gulf of Eilat, maximum 1,850 m under sea level) (Figure 1). The peninsula is divided into three distinct parts: The northern

region consisting chiefly of carbonates, is formed mostly of vast plains and hills covered by sediments all the way to the Mediterranean coast. The central area dominated by the Tih Plateau also drains to the Mediterranean Sea. The southern part, the Precambrian Sinai massif with peaks up to 2,637 m a.s.l. (Mount Saint Catherine) is composed of diverse rocks including volcanics and often intruded alkaline granites that are deeply dissected by numerous wadis (Barron 1907; Abdallah & Abu Khadrah 1976; Bayer *et al.* 1988). Most of these wadis run to the southwestern El Qaa plain bordered by the Gulf of Suez (Figure 1). Tectonically the Gulf of Aqaba is more active than the northern extension of the Red Sea Rift within the Gulf of Suez. This resulted in the formation of a broad coastal plain and a greater accumulation of alluvium on the Suez side (Greenwood 1997). Only the southernmost part of the Gulf of Aqaba coastal plain is widely covered by Quaternary sediments. The investigated study sites include the five wadis of Feiran, Morikh, Timan, Eghshy, and Khashabi (Figure 1). These wadis run subparallel to each other in a NE–SW direction and are incised deeply into Precambrian igneous (75%) and older metamorphic (25%) rocks of the Sinai Mountains. All crystal overburden has been removed, leaving the Precambrian basement with a Quaternary sediment cover (Greenwood 1997). At the southwestern mountain front, extensive alluvial fans have been developed on the adjacent approximately 130 km long and 15–23 km wide El Qaa plain, a plain which dips 2° towards the Gulf of Suez. The plain is mainly composed of Upper Tertiary sediments (Abdallah & Abu Khadrah 1976) and is covered by Quaternary alluvial fans at the wadi outlets (Figures 1 and 2). North of the El Qaa plain, the surface is dominated by a windswept gravel cover devoid of vegetation and wadi channels, except for the pediment areas (Greenwood 1997). South of El Tor (Figure 1), the surface is covered by rippled sand, granite boulders and areas of Nebkha dunes.

All wadis are episodically flooded following rainfall storms during fall and winter. Presently, only extreme floods reach the Gulf of Suez, but most floodwater transmits and infiltrates into the sandy channel bed. Groundwater is available only in the 7 km long Wadi Feiran with numerous date palm trees planted by Bedouin tribes.

The hyper-arid climate of the study area is characterized by hot and totally dry summers and milder winters, both typical for the eastern Mediterranean deserts. The area lower than 2,000 m a.s.l. receives an average precipitation of 25 mm yr^{-1}, mainly during single convective storms in autumn and winter, producing flash floods. The maximum measured rainfall in Southern Sinai was 48.3 mm d^{-1} in Sharm El Sheikh on 17 November 1996 and 20.2 mm d^{-1} in St Catherine on 17 October 1997 (Egyptian Meteorological Authority; see Sherief

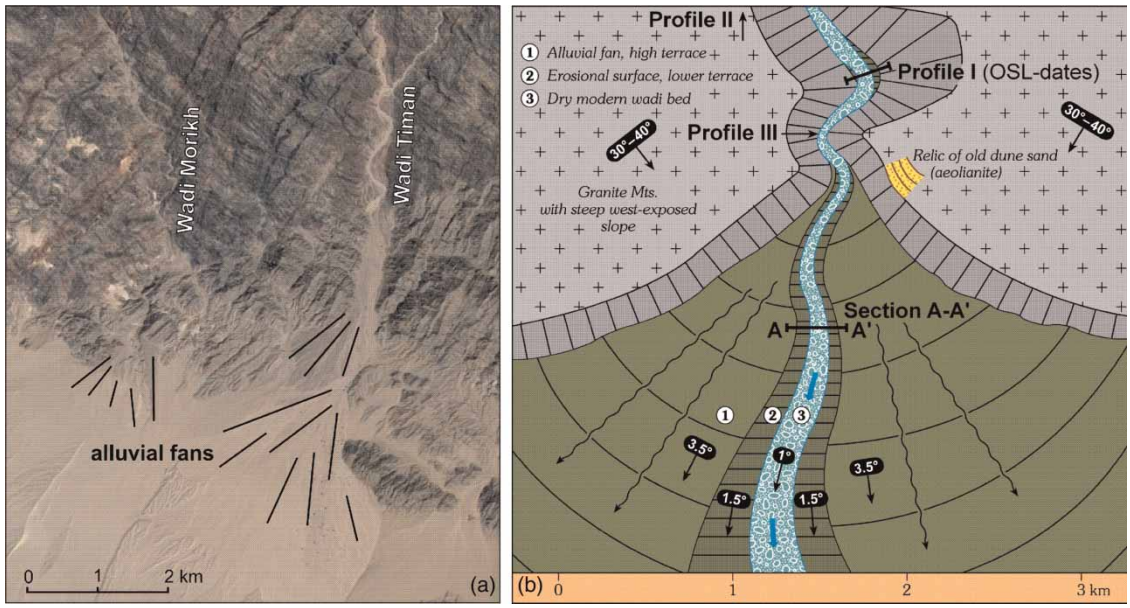

Figure 2 | Alluvial fans. (a) Map section (of Google™ Earth 5.1.3) of the wadi mouths of the Wadis Morikh and Timan. (b) Geomorphic overview near the outlet of Wadi Morikh, indicating the relative location of introduced profiles and sections. The accumulated alluvial fan has been incised by floods during the Holocene.

2008). The October 1997 event is one of the most severe storms associated with an active Red Sea Trough that affected the Negev Desert (Dayan *et al.* 2001; Kahana *et al.* 2002). According to Sherief (2008), the mean annual rainfall ranges between 10 mm yr^{-1} in El Tor, with an orographic increase to 63 mm yr^{-1} in St Catherine (Figure 1). In contrast to the low amount of rainfall, the area is characterized by very high evaporation rates of more than 3,000 mm yr^{-1} (Griffiths 1972). The mean annual temperature exceeds 20 °C in the coastal areas, while on Mt St Catherine it is below 10 °C; frost of −15 °C was measured, and sometimes a snow cover may be observed there (Griffiths 1972; Har-El 1983).

MATERIALS AND METHODS

Sedimentary sections documented here are well exposed along the incised remnants of the fluvial sediments accumulated on the bedrock of the wadi slopes within the mountains. Additional stratigraphy was documented in alluvial fans exposed along channels. In the field, sediment sequences were described and sampled for laboratory analyses. On selected profiles, samples for OSL dating were taken either using opaque sample tubes beaten horizontally into the mostly hard sediments or by the extraction of sediment monoliths (15 × 15 cm).

Each profile and sampling point was located by a handheld global positioning system (GPS). Coordinates are given in Table 1 for each wadi separately.

Sediments were sieved and those of <2 mm separated. Further analyses include grain size distributions, $CaCO_3$ content, total carbon, nitrogen and sulfur contents, as well as pH and electric conductivity (EC, see Table 2). Total contents of iron and manganese were determined by field-portable X-ray fluorescence (FP XRF, NITON XL3t) analysis.

For detailed descriptions of the above-listed laboratory methods, see Völkel (1995) and Hürkamp *et al.* (2009).

Age determinations of 32 samples were measured at The Nordic Center for Luminescence Dating, Risø DK, using the OSL signal from quartz. This signal is particularly sensitive to daylight, and is more readily reset to zero than, for example, the quartz TL signal. After conventional laboratory

Table 1 | Overview of the GPS coordinates of profiles sampled for OSL dating in the several investigated wadis in the Southern Sinai

Profile	OSL	Latitude	Longitude	(m a.s.l.)
Wadi Morikh				
Profile I	OSL 1	28°11′09″N	33°54′38″E	545
	OSL 2	28°11′09″N	33°54′38″E	540
	OSL 3	28°11′09″N	33°54′38″E	533
	OSL 4	28°11′09″N	33°54′38″E	522
	OSL 5	28°11′09″N	33°54′38″E	503
	OSL 6	28°11′09″N	33°54′38″E	510
	OSL 27	28°10′55″N	33°54′34″E	546
Profile II	OSL 8	28°12′21″N	33°54′45″E	658
	OSL 9	28°12′22″N	33°54′46″E	668
Profile III	OSL 10	28°10′35″N	33°54′06″E	467
	OSL 11	28°10′35″N	33°54′06″E	468
	OSL 12	28°10′34″N	33°54′08″E	452
Additional samples	OSL 7	28°10′35″N	33°54′09″E	453
Wadi Timan				
Profile IV	OSL 13	28°12′06″N	33°56′40″E	659
	OSL 14	28°12′5″N	33°56′41″E	648
	OSL 15	28°12′05″N	33°56′41″E	638
Wadi Khashabi				
Profile VII	OSL 16	27°48′55″N	34°12′27″E	81
	OSL 17	27°48′55″N	34°12′27″E	90
	OSL 18	27°48′50″N	34°12′29″E	79
Additional samples	OSL 19	27°48′56″N	34°12′29″E	90
	OSL 20	27°48′56″N	34°12′29″E	85
Wadi Eghshy				
Profile V	OSL 26	28°01′54″N	34°00′32″E	386
Additional samples	OSL 21	28°03′40″N	34°04′00″E	674
	OSL 22	28°03′40″N	34°03′55″E	654
	OSL 23	28°03′26″N	34°03′40″E	565
	OSL 24	28°03′15″N	34°03′20″E	577
	OSL 25	28°01′51″N	34°00′33″E	390
Wadi Feiran				
Profile VI	OSL 28	28°42′10″N	33°58′10″E	1,236
	OSL 29	28°42′10″N	33°58′11″E	1,241
	OSL 30	28°41′54″N	33°58′11″E	1,251
Additional samples	OSL 31	28°41′58″N	33°57′01″E	1,191

Table 2 | Results of physico-chemical laboratory parameters analysis on selected samples of the profiles I (Wadi Morikh) and V (Wadi Eghshy)

			Grainsize * wt. %																				
Profile	Sample	Depth (cm)	cS	mS	fS	Sand	cSi	mSi	fSi	Silt	Clay	Soil[a] Texture	pH $CaCl_2$	pH H_2O	EC µS cm^{-1}	$CaCO_3$ %	Munsell Color	OC %	TC %	OM %	TN %	TS %	Fe %	Mn Ppm
I (unit 3)	1	250	2.0	69.8	23.8	95.7	1.7	1.6	0.1	3.4	0.9	mSfs	8.2	8.1	1,810	12.2	10YR 5/4	0.09	1.07	0.1	0.02	0.08	0.46	399
I (unit 3)	2	800	2.0	34.9	50.9	87.8	5.7	1.4	1.8	9.0	3.2	fSms	8.8	8.3	357	17.8	10YR 5/6	0.02	1.83	0.0	0.01	0.17	0.72	<LOD
I (unit 3)	2a	750	16.1	31.6	31.0	78.7	11.0	3.1	1.5	15.7	5.6	gGr/Sl2	8.1			20.1	10YR 5/6	0.09	1.77	0.1	0.02	0.20	0.88	<LOD
I (unit 2)	3	1,500	0.0	3.4	72.9	76.3	16.8	2.2	1.0	20.0	3.7	Su2	8.2	8.7	256	26.0	10YR 5/4	0.04	2.64	0.1	0.01	0.04	1.04	<LOD
I (unit 2)	4	2,570	0.1	38.9	48.5	87.5	7.1	1.4	1.2	9.7	2.8	fSms	8.2	8.6	42	19.2	10YR 5/6	0.03	1.96	0.0	0.01	0.03	0.79	<LOD
I (unit 1a)	5	4,500	4.4	40.1	50.0	94.5	3.0	2.2	1.5	6.7	0.0	fSms	8.1	8.7	97	18.3	10YR 5/4	0.02	1.78	0.0	0.01	0.02	0.95	<LOD
I (unit 1b)	6	3,800	1.5	12.3	65.6	79.4	15.7	1.7	1.1	18.6	2.0	Su2	8.1	8.7	120	22.3	10YR 5/4	0.07	2.24	0.1	0.01	0.02	0.87	<LOD
IV	7												8.0			40.9	10YR 5/4		4.00		0.01	0.03	0.98	249
V	8	0–30	18.0	29.1	37.3	84.4	4.6	1.9	2.9	9.4	6.2	St2	7.6			1.8	7.5YR 5/8	0.02	0.10	0.0	0.01	0.03	1.81	324
V	9	30–60	28.2	24.8	36.0	89.1	4.7	2.1	2.7	9.6	1.4	fSgs	7.7			2.0	7.5YR 5/6	0.01	0.08	0.0	0.01	0.04	1.81	318
V	10	60–90	62.1	15.4	10.0	87.5	4.3	3.3	2.8	10.5	2.0	Su2	7.7			2.0	7.5YR 5/6	0.01	0.08	0.0	0.01	0.03	2.65	428

[a]According to ad-hoc AG Boden (2005).

cS, coarse sand; mS, medium sand; fS, fine sand; cSi, coarse silt; mSi, medium silt; fSi, fine silt; EC, electric conductivity; OC, organic carbon; TC, total carbon; OM, organic matter; TN, total nitrogen; TS, total sulfur; LOD, limit of detection.

acid treatment to extract a clean quartz-rich extract, 180–250 μm grains were mounted on 9.8 mm diameter stainless steel disks using silicone oil for subsequent luminescence measurement using a Risø TL/OSL Reader model DA20 (Bøtter-Jensen *et al.* 2003). The OSL signal was stimulated using blue (470 nm) light emitting diodes, and detected through a U-340 glass filter. OSL signals were regenerated using a calibrated beta source mounted on the reader. A single aliquot regenerative-dose (SAR) protocol (Murray & Wintle 2000) was used with a 260 °C preheat for 10 s, a 220 °C cut heat, and a clean out step using blue light stimulation while the sample was held at 280 °C (Murray & Wintle 2003). The OSL signals were dominated by the quartz fast component (Jain *et al.* 2003; Singarayer & Bailey 2003), and the dose recovery test (used to test the applicability of the chosen protocol) gave a measured to given dose ratio of 0.95 ± 0.02 ($n = 24$), demonstrating that our SAR protocol is able to measure a known dose given to an optically bleached sample of this material before any thermal treatment.

Dose rates were measured on ~250 g subsamples taken from immediately adjacent to the OSL samples. These were crushed, cast in wax in a well-defined geometry, and analyzed using high resolution gamma spectrometry (Murray *et al.* 1987) after 3 weeks' storage to allow ^{222}Rn to reach equilibrium with its parent ^{226}Ra. Radionuclide concentrations were converted to dose rates using tabulated data (Olley *et al.* 1996) and a cosmic ray contribution was based on Prescott & Hutton (1994). The lifetime water contents are assumed to be the average of the laboratory saturated values and those observed at the time of sampling; they are expressed in % of dry weight. All relevant OSL data are summarized in Table 3.

RESULTS

Investigations were carried out on sediment profiles in five wadis of the southwestern Sinai Mountain edge, focusing on the fluvial and eolian wadi fills that are also marked as erosional scarps on both valley slopes (Figures 2–6). For comparison, some sediment profiles in the canyon-like middle reaches of Wadi Feiran were studied. In all other wadis, generally the central to lower sections and the proximal part of the corresponding alluvial fan were investigated. A focus on Wadi Morikh provided detailed chrono-stratigraphic results.

Wadi Morikh

Wadi Morikh has a catchment area of 74 km^2 with its highest point at 1,057 m a.s.l. The sediment filling on the base of the narrow wadi consists of fluvially deposited, well-rounded granite boulders and gravel, covered by eolian sands and silts. On the valley slopes, interbedded finer-grained sediments (gravel to clay) are exposed in fluvially cut scarps. The existence of erosional sediment remnants in Wadi Morikh can be traced at least 5 km up its mouth (Figure 2). The thickness of these deposits reaches 40 m at the wadi outlet (Figures 3–5). Two fluvial terraces are evident in the lower 5 km of Wadi Morikh, a lower terrace of approximately 6 m and an older terrace 20–40 m above the modern channel (Figures 4 and 6). The terrace top level is traced to and associated with a corresponding alluvial fan at the wadi mouth and covers the pediment at the mountain front (Figure 2). The alluvial fan slope has low inclination angles around 1° at the base, but angles rise towards the top of the fan up to 3.5° (Figure 3). Its total length of 7 km (united with the fan of Wadi Timan) is comparatively short. The sediment on top of the terrace and the alluvial fan mainly consists of large granite angular to sub-rounded boulders and gravels that become smaller in size in the distal parts of the alluvial fan. The boulders often show ventifacts. Below the surface, the sediment character changes to finer material, this is a recurring sedimentologic component of the central part of the fan. Recently, deep incision cut a channel into the alluvial fan; it reveals sedimentary sequences and layering with different inclinations of the near-surface and basal layers. At the bottom, lower angles are developed compared to the top; this indicates an extremely high sediment load during alluvial fan accretion (Figure 3).

A typical profile of the fluvial deposits 1 km into the watershed is exposed on the southeastern valley slope. Profile I (Figures 4 and 5) is 51.2 m thick and is from bottom to top as follows (sample numbers according to OSL numbers, see Table 3).

Unit 1a (Figures 4 and 5) consists of angular, poorly adjusted clasts up to 20 cm in diameter and yellowish

Table 3 | Results of OSL age determinations

Sample	Wadi	(m a.s.l.)	Depth (cm)	Elev.[a] (cm)	Age (ka)	Dose (Gy)	*n*[b]	Dose rate (Gy ka^{-1})	w.c.[c] (%)	Risø No.
OSL 1	Morikh	545	250	4,700	24.6 ± 1.7	49 ± 2	18	2.00 ± 0.10	0	07 54 01
OSL 2	Morikh	540	800	4,400	27.4 ± 1.7	59.2 ± 1.8	18	2.16 ± 0.11	0	07 54 02
OSL 3	Morikh	533	1,500	3,400	34 ± 2	84 ± 4	17	2.48 ± 0.13	0	07 54 03
OSL 4	Morikh	522	2,570	2,300	32 ± 2	81 ± 4	18	2.54 ± 0.13	0	07 54 04
OSL 5	Morikh	503	4,500	200	43 ± 3	81 ± 3	16	1.89 ± 0.10	0	07 54 05
OSL 6	Morikh	510	3,800	700	38 ± 2	109 ± 4	18	2.87 ± 0.15	0	07 54 06
OSL 7	Morikh	453		200	37 ± 2	71 ± 2	18	1.94 ± 0.10	0	07 54 07
OSL 8	Morikh	658		500	46 ± 3	151 ± 4	25	3.29 ± 0.16	2	08 54 14
OSL 9	Morikh	668		1,500	42 ± 3	137 ± 7	25	3.26 ± 0.10	2	08 54 15
OSL 10	Morikh	467	70	1,240	43 ± 3	82 ± 2	25	1.90 ± 0.09	2	08 54 16
OSL 11	Morikh	468	440	800	54 ± 3	90± 2	26	1.65 ± 0.08	2	08 54 17
OSL 12	Morikh	452	500	100	36 ± 2	89 ± 3	26	2.50 ± 0.12	2	08 54 18
OSL 13	Timan	659		2,400	23.9 ± 1.6	135 ± 6	24	5.65 ± 0.27	2	08 54 19
OSL 14	Timan	648		1,270	30 ± 2	181 ± 10	24	6.02 ± 0.29	2	08 54 20
OSL 15	Timan	638		300	29.5 ± 1.9	161 ± 6	27	5.47 ± 0.26	2	08 54 21
OSL 16	Khashabi	81		100	87 ± 8	116 ± 9	27	1.33 ± 0.07	2	08 54 22
OSL 17	Khashabi	90		1,200	12.7 ± 0.9	27.2 ± 1.2	25	2.14 ± 0.10	2	08 54 23
OSL 18	Khashabi	79		30	97 ± 6	171 ± 5	27	1.76 ± 0.09	2	08 54 24
OSL 19	Khashabi	90		600	44 ± 3	70 ± 3	27	1.59 ± 0.08	2	08 54 25
OSL 20	Khashabi	85		100	53 ± 3	116 ± 4	25	2.20 ± 0.11	2	08 54 26
OSL 21	Eghshy	674	30		18.8 ± 1.2	98 ± 3	24	5.19 ± 0.25	2	08 54 27
OSL 22	Eghshy	654	120		46 ± 4	176 ± 10	18	3.80 ± 0.18	2	08 54 28
OSL 23	Eghshy	565	20	370	47 ± 3	205 ± 9	27	4.32 ± 0.21	2	08 54 29
OSL 24	Eghshy	577		200	30 ± 3	141 ± 14	22	4.72 ± 0.22	2	08 54 30
OSL 25	Eghshy	390	500	100	52 ± 3	131 ± 4	19	2.53 ± 0.12	2	08 54 31
OSL 26	Eghshy	386	380	100	55 ± 3	99 ± 3	26	1.80 ± 0.09	2	08 54 32
OSL 27	Morikh	546	180	4,900	19.3 ± 1.3	44 ± 2	24	2.28 ± 0.11	2	08 54 33
OSL 28	Feiran	1,236	600	30	25.9 ± 1.9	135 ± 7	20	5.22 ± 0.25	2	08 54 34
OSL 29	Feiran	1,241	160	500	8.4 ± 0.7	67 ± 4	23	7.93 ± 0.38	2	08 54 35
OSL 30	Feiran	1,251	40		8.9 ± 0.6	44 ± 2	27	5.00 ± 0.24	2	08 54 36
OSL 31	Feiran	1,191	380	30	47 ± 3	132 ± 2	26	2.81 ± 0.14	2	08 54 37

[a]elev. = elevation above wadi floor.
[b]*n* = number of aliquots measured.
[c]w.c. = mean estimate water content.

brown sands. Silt is present in minor amounts (<7 wt. %). Clay is missing. The dominating grain size of the fraction <2 mm is fine (50 wt. %) and medium (40 wt. %) sand. The carbonate-cemented (18% carbonate) sediments are well stratified. The layers are 5–25 cm thick and are laterally replaced by bands of pure coarse sand. The layers and lenses have different angles and directions. The basal sediments at 45 m depth top are 43 ± 3 ka (OSL 5, Figures 4 and 5, Table 3).

Unit 1b is similar to 1a and consists of slightly smaller angular clasts, which are partly adjusted by sedimentation processes. The amounts of sand (66 wt. % fine sand) and silt (20 wt. %) increase towards the top of unit 1b. The sediments are cemented by microcrystalline calcite and contain

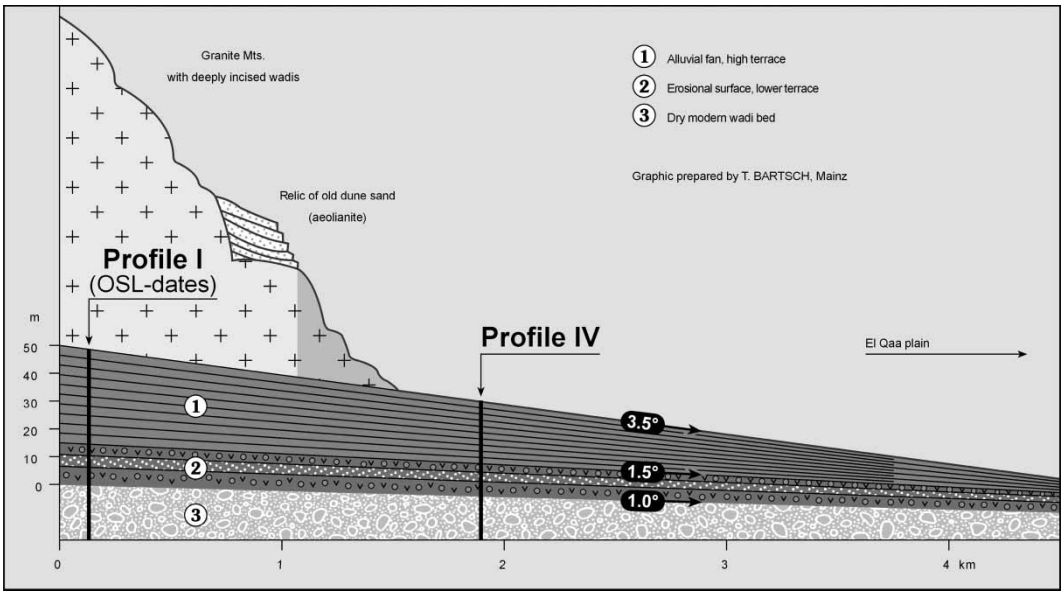

Figure 3 | Geomorphic overview of the fan in Wadi Morik as seen from the actual wadi bed. View direction is towards the south. Low angle bedding is developed at the bottom, steeper angles towards the top which indicate relatively rapid sedimentation during the fan formation. This happened synchronously with the accumulation of the upper terrace inside the valley. Ongoing fluvial erosion has been the dominating process until today.

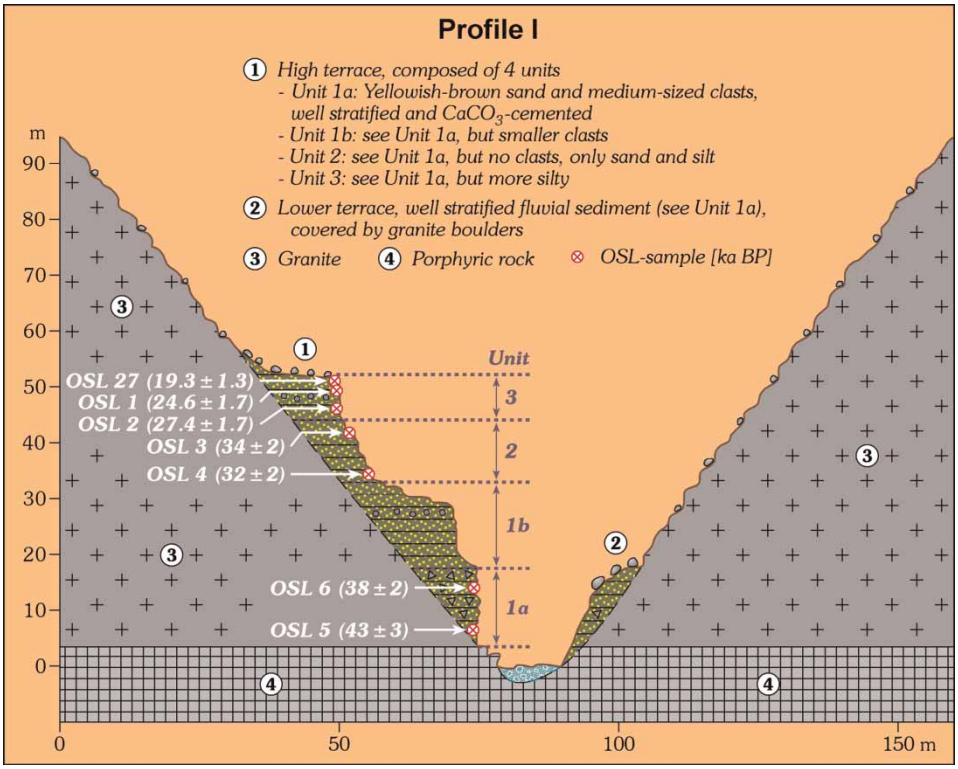

Figure 4 | Detailed geomorphic and stratigraphic section at the location of profile I in the Wadi Morikh (compare also Figure 5, which shows a photograph of this section). Heights and location of the different stratigraphic units as described in the text, are given together with OSL dates (compare Table 3).

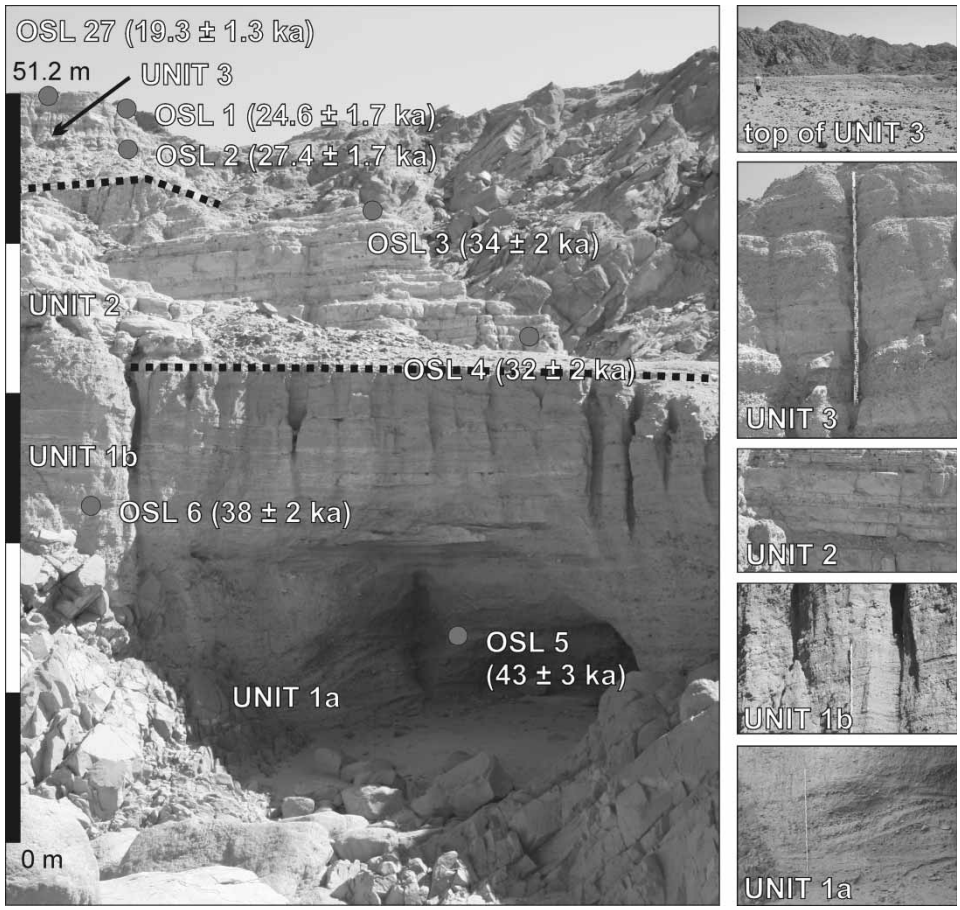

Figure 5 | Photograph of profile I in the lower reaches of Wadi Morikh with location of the OSL sampling points and determined ages. Three different sediment units based on fluvial and eolian sedimentation are developed.

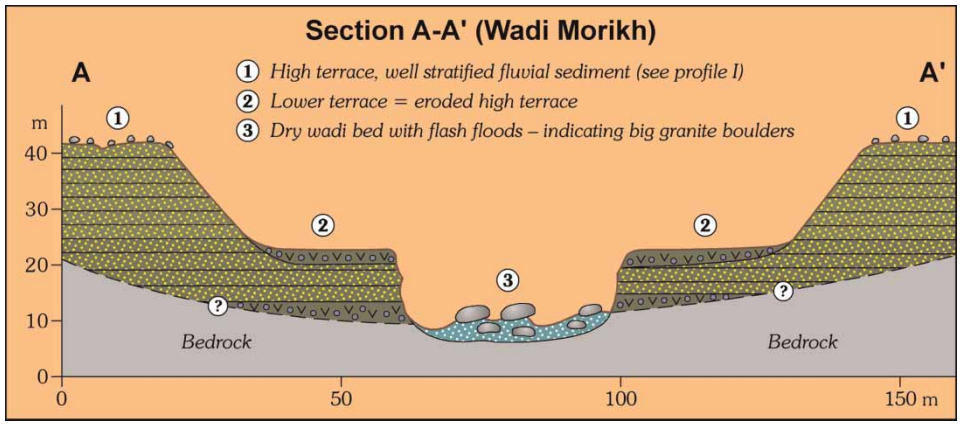

Figure 6 | Section A–A′ at the beginning of the fan in the Wadi Morikh (location compare Figures 1 and 2(b)). The high terrace in the lower reach of the wadi corresponds with the highest level of the fluvial fan.

>22% carbonate. The bedding is (sub)horizontal. Layers of pure sand and silt frequently cover or underlie the typical coarser deposits. The inclination of the bedding is parallel to the valley, which can be partly followed along hundreds of meters. The age of these deposits at a depth of 38 m is 38 ± 2 ka (OSL 6, Table 3) in profile I (Figures 4 and 5).

Unit 2 consists of mainly silt to sand. The amount of silt increases from 10 wt. % at the base to 20% at the top (Table 2). The fine sand at the top changes with depth from fine to medium sand, with similar proportions in both grain size fractions. No coarse or larger clasts were identified. Silty layers up to 30 cm thick are separated by sand layers, each up to 10 cm in thickness. The sediments are partly cemented (26–20% $CaCO_3$) and probably of eolian origin and fluvial reworking. Unit 2 is dated at the base (25.7 m depth) and at the top (15 m depth) to 32 ± 2 and 34 ± 2 ka (OSL 4, 3), respectively. Both ages are within errors.

Unit 3 consists of layers alternating between coarser and finer sediments. The sediments are less cemented compared to units 1 and 2 despite a nearly equal carbonate content of 18%. The smaller grade of cementation could be the reason for low water contents during sediment accretion. The coarse sediments, which can be as large as 30 cm, consist of angular and partly rounded clasts up to a minimum of 5 cm in diameter. They are mixed with sediments finer than 2 mm (70 wt. % medium sands, 24 wt. % fine sands). Fine sediment bands, up to 10 cm thick, consist mainly of fine sand (51 wt. %) and silt. The clasts are horizontally adjusted. At a depth of 7.5 m from the top, a coarse gravel layer is exposed (sample 2a, Table 2). In contrast to the over- and underlying sediments, the <2 mm fraction in this layer is composed of equal amounts of medium to fine sand. However, in addition, 16 wt. % portions of coarse sand as well as silt are determined. Therefore, the sediment possesses the most heterogeneous texture distribution classified for profile I. Sulfur contents of 0.2% are probably evidence of minor amounts of gypsum. Electric conductivity of 1.8 mS cm^{-1} in the surficial layer, indicating higher salt contents, is probably part of a soil formation (Amit *et al.* 1993, 2006) in this hyper-arid environment. The layers at the base of unit 3 are 27.4 ± 1.7 ka (OSL 2) and those at the top 24.6 ± 1.7 ka (OSL 1) and 19.3 ± 1.3 ka (OSL 27). A desert pavement is remarkably well developed on top of unit 3 (Figures 4 and 6).

Two additional profiles were documented and dated in this basin. In profile II (Figures 2(b) and 7(b), location see Table 1) fluvial sediments of the central valley of Wadi Morikh 2.5 km upstream of profile I are exposed in approximately 30 m thick deposits (Figure 7(a)). At the base, calcareous silt layers are interbedded with gravels. The silts are 46 ± 3 ka (OSL 8). At the top, similar sediments provide an age of 42 ± 3 ka (OSL 9).

Profile III (Figures 2(b) and 7(c)) is located near the wadi mouth (location see Table 1). The top of the profile is 26.3 m above the wadi floor. At the profile base, 8 m above the wadi floor, 4.4 m of eolian sediments were accumulated, secondarily cemented, and partially buried. This is a fossil dune overlying the fluvial sediments within the lower reaches of Wadi Morikh. Except for Khashabi Wadi and a single, spatially limited eolianite in Wadi Eghshy, such sediments have not been found in any of the other wadis. They are more common at the proximal parts of the El Qaa. Recent and apparently active sand dunes cover many of the lee-side bedrock slopes at the mountain front and form numerous small nebkas on the desert coastal plain. The age of the eolian sediment in Wadi Morikh (Figure 7(c)) is 54 ± 3 ka (OSL 11) at the base and 43 ± 3 ka (OSL 10) on the top, respectively. Below the yellowish dune sediments a sharp discontinuity to brownish, coarse base gravels is exposed. They are angular and marginally sorted. Despite their different age of >54 ka the gravels of profile III in Wadi Morikh can be correlated to unit 1a of profile I. Similarly, the dune sediments are comparable with unit 2 in profile I. Unit 1b is missing in profile III. On the other side of the valley floor, directly opposite to profile III, an eolianite is buried by more than 10 m of interbedded coarse- and fine-grained fluvial deposits. The top of the fossil dune has been dated to 36 ± 2 ka (OSL 12), which is younger than the paleodune in profile III but comparable in age to unit 2 in profile I.

Wadi Timan

The fluvial sediments of Wadi Timan (93 km^2, 38 km long) are similar to those of Wadi Morikh with regard to their thickness and spatial distribution within the valley (Figure 1). Generally, the grain size is somewhat coarser and pure eolian components are missing. In profile IV some 2.5 km upstream of the wadi outlet, an approximately 25 m high fluvial sediment was sampled for OSL dating. The intensely carbonate cemented deposits were accumulated between 24 and 30 ka (OSL 13–15, Table 3). Sediments 3 m above the wadi floor and of 13 m height provided almost the

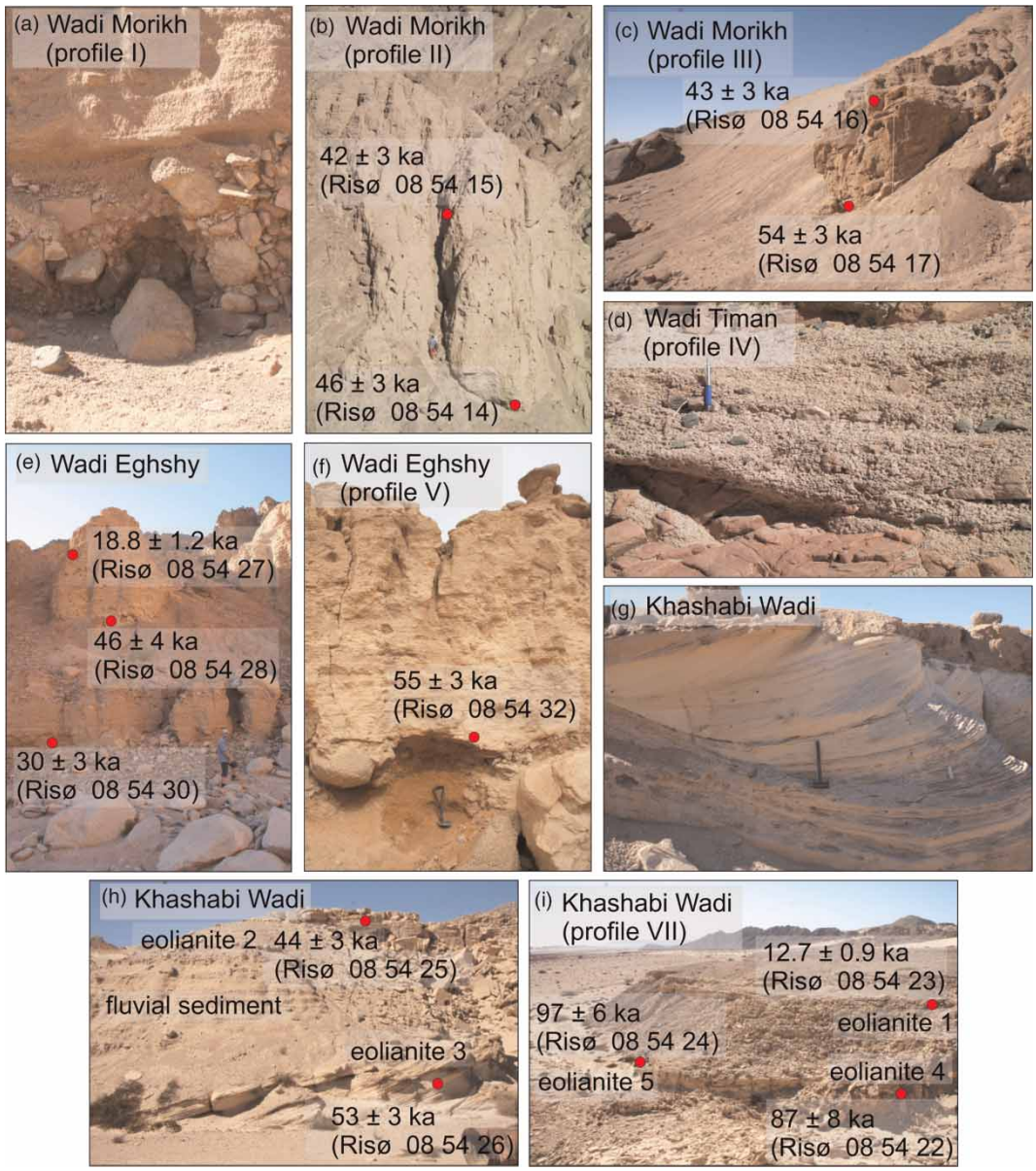

Figure 7 | Examples of different (sometimes OSL dated) sediment types. (a) Angular to subrounded fluvial gravels and boulders below the eolianites (fossil dune) in the lower reaches of Wadi Morikh (profile I). (b) Erosional scarp of profile II with sequence of fluvially deposited upper terrace sediments in the middle to upper reaches of Wadi Morikh. (c) OSL dated eolianite block of profile III on top of the fluvial terrace sediments in the lower reaches of Wadi Morikh. (d) Calcretized basal conglomerate in Wadi Timan. (e) Fluvial deposits in Wadi Eghshy. OSL samples 21 and 22 date the upper terrace, OSL 24 is situated in accreted sediments of the lower terrace covering calcretized clasts at the base. There is a big difference in age between OSL 21 and 22, but no clear unconformity has been detected within the sediment body. (f) Paleosol and overlaying OSL dated eolianites in the Wadi Eghshy (profile V). (g) Cross-bedded eolianites in the Khashabi Wadi near Sharm El Sheikh. (h) and (i) Profile VII provides the interbedding of five OSL dated eolianite bodies with fluvial sediments in the Khashabi Wadi.

same age. It seems that the deposits 3 m above the wadi floor were accreted later or belong to the lower fluvial terrace.

In Wadi Timan, the basal gravels that are overlain by the fine-grained fluvial sediments (see above) are well exposed at 28°13′09″N and 33°57′08″E. The layer is strongly consolidated by carbonate (>40% $CaCO_3$ in the matrix), consists of >70 wt. % rounded to subrounded gravels (in contrast to Wadi Morikh) and is conglomeratic (sample 7 in Table 2, Figure 7(d)).

Wadi Eghshy

Contrary to the other wadis, in the 22 km long Wadi Eghshy (145 km^2) sediments are only preserved in the lower reaches. Two fluvial terraces are distinguished. The upper terrace merges to the alluvial fan surface outside the valley gorge. The proximal part of this uneroded alluvial fan and the uppermost layers of the higher terrace level slope is 3°. In the lower valley section, the lower terrace is 3.8 m above the wadi floor. The sediments on top, in the middle and at the base of the upper terrace, are 18.8 ± 1.2 ka (OSL 21), 46 ± 4 ka (OSL 22), and 30 ± 3 ka (OSL 24) (Figure 7(e)). Slack-water deposits in a small bedrock shelter near the wadi mouth and 3.70 m above the wadi floor are 47 ± 3 ka (OSL 23).

In a small tributary incised in a granitic bedrock near the mouth of Wadi Eghshy (profile V, Table 1), fluvial gravels and sands interfinger with eolianites, overlaying a thin layer of the typical basal gravels, which bury a paleosol (Figure 7(f)). The paleosol can be well distinguished from the over- and underlying sediments by its more brownish color, and initial formatted soil aggregates. Beneath the soil, the granitic bedrock crops out. Except for this location, no eolian sediments were accumulated within the gorge. This brownish soil remnant has been sampled by dividing weakly developed cambic horizons each of 30 cm thickness (samples 8–10, Table 2). The uniform color of the cambic horizon is of a distinct difference compared to fine laminated color contrasts often found in the fluvial sediments. The amount of gravel increases with depth from 34 to 73 wt. %. The grain size of the matrix is silty and clayey sand, respectively, in the uppermost layer. The sand fraction changes with depth from a fine to a coarse sand. The portions of silt only slightly increase, clay contents distinctively decrease from >6 to <2 wt. %. pH index is about 7.7, and carbonate contents are relatively low (2%). The color of the soil is bright brown. The development of uniformly dispersed manganese, as well as iron oxides and hydroxides, is expressed in a higher amount of total iron and manganese (1.8% Fe in the uppermost 60 cm, 2.6% Fe from 60 to 90 cm depth, >300 ppm Mn). Two samples provide identical ages of 52 ± 3 ka (OSL 25) and 55 ± 3 ka (OSL 26).

Wadi Feiran

Wadi Feiran is 143 km long and, therefore, the largest (620 km^2) of all wadis in South Sinai. It originates in the most elevated area of Mt. St. Catherine (2,637 m a.s.l.), which is at present affected by the Mediterranean climate zone. This should be taken into consideration when the paleoclimatic conditions are discussed. Wadi Feiran is the only basin in the area where previous investigations and age determinations on the Quaternary sediment fills were carried out, mainly on the thick and fluvially relocated eolian sediments of its middle reaches. In profile VI (location see Table 1) and near Oasis Tarfat at the wadi of El Sheikh (Figure 1), the top layers of the sediment fill are exposed. The location east of Tarfat is near where earlier TL ages were provided for profile XI, described by Smykatz-Kloss *et al*. (1998) and Rögner *et al*. (1999, 2004). Our new OSL samples were taken from homogenous silt to fine sand in the higher mountainous reaches of Wadi Feiran (~1,240 m a.s.l.; Figure 1). The ages range between 8.4 ± 0.7 ka (OSL 29) as well as 8.9 ± 0.6 ka (OSL 30) at the top and 25.9 ± 1.9 ka (OSL 28) in the basal fine sands of profile VI, only 30 cm above the wadi floor. In a small tributary valley (Wadi El-Dallal), a few kilometers further downstream, silty deposits in the wadi bed with calcareous nodules are interbedded with gravelly fluvial deposits. An unconformity at the base marks the transition to the underlying sands. The silts provide an age of 47 ± 3 ka (OSL 31).

Khashabi Wadi

Khashabi Wadi is located at the southernmost headland of the Sinai Peninsula. Multiple exposures of cemented eolianites are widespread in the 17.6 km² wadi basin (Figures 7(g) and 7(i)). Profile VII (location see Table 1) spans a length of 200–300 m at the western valley slope and is 5–6 m high. The top and basal parts of the eolianites were sampled for OSL ages (Figures 7(h) and 7(i)). In total, five eolianite bodies can be distinguished. Sample OSL 18 of the oldest sediments is 97 ± 6 ka. The eolian sediment is embedded by fluvial sediments and again underlain by another eolianite sampled in OSL 16, which provides an age of 87 ± 8 ka. The overlying eolian sand/silt body is

12.7 ± 0.9 ka old (OSL 17) and represents the highest-located and youngest eolianite in this profile and probably in the entire study area. Additional eolianites were sampled at an adjacent terrace profile 1 m and 5–6 m above the wadi floor (OSL 20, 19). They were dated to 53 ± 3 and 44 ± 3 ka, respectively.

DISCUSSION

The studied wadis show a similar pattern in their late Quaternary sediment fills. Different sediment textures and spatial distributions within the narrow wadis resulted from fluvial torrents, slack-water deposition, and/or eolian deposition. Fluvially rounded granite boulders are interbedded with angular clasts that indicate transports over short distances, probably from the adjacent valley side slopes. Additionally, large quantities of silt to fine sand eolian sediments were accumulated with these deposits and subsequently fluvially reworked. Furthermore, partially stabilized and fossilized sand dunes were deposited in places on top of the fluvial sediments in the lower reaches of the valleys, where they are open to the El Qaa plain (Figure 2(b)). In recent times, dunes still form on the lee sides of the mountain slopes adjacent to the coastal plain.

During the winter season the prevailing wind direction in south Sinai is NNW following the western borderline of the high mountains massif. Strong winds sometimes combined with sandstorms are frequent in January and February (Kahana *et al.* 2002; Sherief 2008).

The sediments can be distinguished based on their age and origin:

1. The deposits predate or underlie the fluvial and eolian sedimentary valley fills. These are gravel and conglomerate layers, documented in Wadis Morikh and Timan as well as the cambic paleosol underlying a thin bed of basal gravels in Wadi Eghshy (Figure 7(f)). Neither the basal layer nor the paleosol could be dated due to the lack of dateable material. A minimum age for cambic soil can be estimated from the OSL ages of the overlying strata. The eolian transport, which initiated the accumulation of the yellowish eolianites on top of the cambic soil and the overlying gravels in Wadi Timan, started >55 ka (OSL 26, Table 3, Figure 7(f)). Therefore, the deposition of the basal gravels as well as the pedogenesis predate this age. It must have been a period with slightly more continuous moisture than today and a reduced geomorphodynamic system in order to allow a weak but well distinguishable cambic soil. The climate must have been slightly more semi-arid with rainfall towards 100 mm yr^{-1} as is actually the case in North Sinai and the Negev region (Greenwood 1997; Greenbaum *et al.* 2000, 2006; Sherief 2008).
2. In the Wadis Morikh, Eghshy and Feiran, basal fine-grained sediments are dated to 46–47 ka (OSL 8, 22, 31, Table 3). This indicates a consistent contemporaneous onset of at least episodic water flow in the wadis after 50 ka. Before they accumulated, any former wadi fills – if they ever existed – must have been totally eroded, because in most cases the alluvial sediments directly cover the granitic bedrock (see also Figure 5).
3. Otherwise, fossil dunes overlie the igneous rock basement as in Wadi Eghshy, dated to 55–52 ka, or in Wadi Morikh, dated to 54 ka (compare Figure 7(b)). This indicates a more windy period before a reactivation of more frequent flooding processes. The fluvial sediments are composed of gravelly layers and intermittent with eolian deposits, which are secondarily consolidated by carbonate and thus transformed into eolianites (sediment group c).

The well-preserved eolianites of the Khashabi Wadi at the southernmost point of the Sinai Peninsula near Sharm el Sheikh provide evidence of a continuous eolian deposition throughout the last 100 ka due to a supposedly persistent hyper-arid climate (Figure 8(c)). Fluvial and eolian sediments were likewise deposited between 45 and 35 ka in the Wadi Morikh, indicating that phases of fluvial and eolian activity must have occurred contemporaneously or at frequent intervals, respectively (Figures 8(a) and 8(b)). A continuous eolian activity under strong winds in winter and periodically discharging floods implement sedimentation and erosion processes with a general tendency to accumulation caused by variations within an arid climate. In a comparable record of the southern Negev Desert in Israel, Greenbaum *et al.* (2006) compiled 27 large paleofloods between 33 and 29 ka in a slack-water deposit profile, attributed to increased frequency of a seasonally

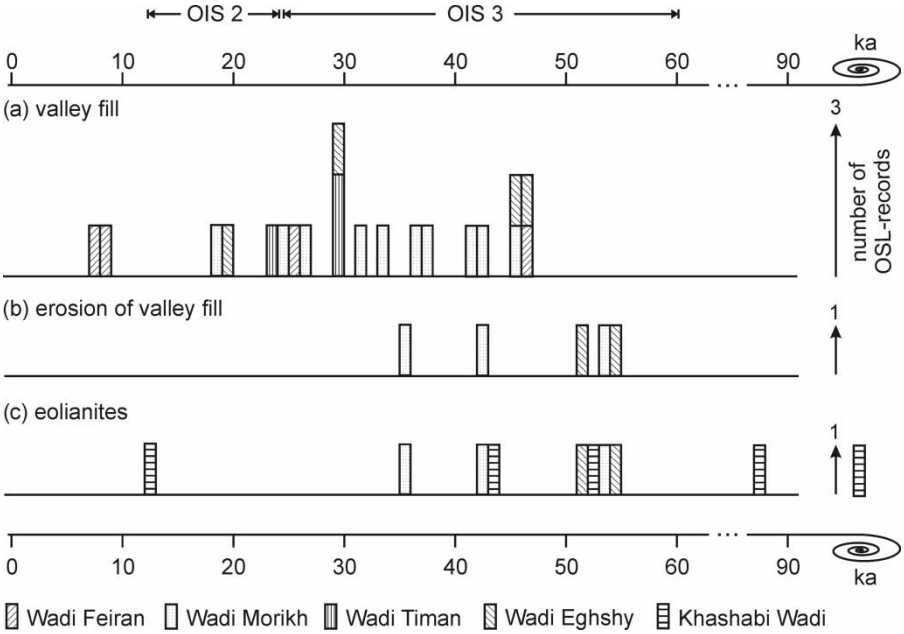

Figure 8 | Chronological overview of determined OSL records of all investigated wadis, distinguished into three groups of sediments, which represent (a) wadi fillings, (b) erosion phases and (c) eolianites and therefore indicate different paleoclimatic conditions.

intensified low-pressure system affecting that area by heavy rainfalls generated by the invasion of tropical air masses. This system could have been induced by a temporarily stronger active Red Sea Trough or its more frequent occurrences as postulated by Dayan & Morin (2006), Kahana *et al*. (2002) and Sherief (2008). Mediterranean climate systems within predominantly temperate air masses led to wetter conditions between 40 and 20 ka, indicating a semi-arid climate with a supposedly lower level of mean temperatures than today. This points to a potentially synchronous strengthening of both climatic phenomena during MIS 3 and towards the LGM (MIS 2).

A similar interpretation is given for an up to 30 m sedimentary fill in Wadi Sabra, South Jordan, which is, therefore, well comparable to that of the South Sinai valleys (Bertrams *et al*. 2012). According to them, 'a phase of continuous aggradation was active from at least 30 ka onwards, leaving more or less homogeneous fluvial and fluvio-eolian sand deposits. These are interpreted to be the result of a local climatic regime inducing higher sediment-supply and lower runoff intensities than today which might have been caused by higher amounts of snowfall in precipitation or generally a more balanced seasonal rainfall pattern'. The OSL dates range from 30 to 15 ka (MIS 3 and 2) which means between the dates of Wadi Feiran and the other South Sinai wadis.

There is another remarkable similarity between the South Sinai valleys and Brachina valley in the Flinders Ranges of semi-arid South Australia (Glasby *et al*. 2010; Haberlah *et al*. 2010a, 2010b). The authors used multi-proxy analyses and, therefore, described the composition and chronology of a fine-grained late-Pleistocene valley-fill in great detail: it is 7–9 m thick and formed predominantly between 24 and 18 ka (extended LGM; Mix *et al*. 2001). Several stages of late Pleistocene environmental changes are distinguished:

- Before 34 ka episodic aggradation and erosion were the dominating processes. Accumulation of basal lag gravels later transformed into a conglomerate by $CaCO_3$-infiltration.
- From 34 to 25 ka, more humidity creates a denser dust-trapping vegetation on the slopes.
- From 25 to 21 ka, a decrease in vegetation density and increase of dust flux due to a drier and cooler climate, respectively.

- From 21 to 17 ka, a cool, dry and windy climate prevailed. This produced suspension load flows in the valleys and the aggradation of fine sediment.
- Overall incision started at 17 ka, induced by an, again, warmer and wetter climate.

The first-order dust peaks around 32 and 21 ka were characterized by the coexistence of dust storms and episodic floods. This fundamental result, being transmitted to the South Sinai wadis, may help to understand the aggradation dynamics of the described, very thick and mostly fine-grained sediments.

Kehew *et al.* (2010) reconstructed discharge values in Wadi Isla (Southern Sinai, Figure 1) on the basis of the transport of large boulders of 2 m diameter present in the lower reaches of the wadi. They yield discharges of ~1,600 $m^3 s^{-1}$ and velocities of 6.8–7.3 $m s^{-1}$, indicating a corresponding storm precipitation range of 100–125 mm. This is about three times higher than the maximum rainfall recorded at Sharm El Sheikh in 1966 and seems, therefore, unrealistic. Additionally, no oral tradition for such a large flood exists with the local bedouin tribes. Large wadi flash floods are either rich in suspended matter or are close to debris flows; this could largely increase the carrying capacity of the flows. The overall movement of boulders downstream may be activated by a relatively low discharge.

Three different sediment units can be distinguished within the South Sinai wadis (compare also Figures 4 and 5). They are interpreted as follows: Debris flows deposited along the gorge and genetically are disconnected to the valley sides nearby. For example, unit 1a (Figures 4 and 5) can be interpreted as a debris flow which relocated only a short distance. During the accumulation of unit 1a (~45–35 ka), the instantaneous sedimentation rate (of these angular clasts) was very high (1.40–2.50 $m yr^{-1}$, see Figure 9). Also, for unit 1b, the transportation distance of the sediments must have been short due to the angular shape of the rocks. Compared to unit 1a, the size and number of the clasts, as well as the increase in finer material indicate a change in the amount of water and, maybe, eolian sand deposition on the slopes that later redeposited.

The sediments of unit 2 differ drastically from those of unit 1a and 1b. No fragments >2 mm were found. The sediments are of pure eolian origin, and subsequently relocated

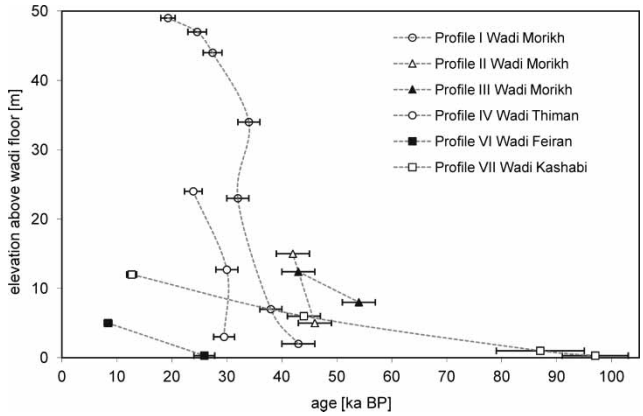

Figure 9 | Depth–age diagram of selected sediment profiles in different wadis. Steep curve shapes indicate rapid sedimentation, gently inclined curves imply low sedimentation rates. Increased sediment deposition is documented for the time period 30–50 ka (MIS 3) for Wadi Morikh (profiles I and II) as well as Timan (profile IV).

by water. As both types of sediments (units 1 and 2) can be found in the valley fills and the alluvial fan at the wadi mouth, the differences in the sediment types are interpreted as changes in the processes of sediment sources, bedrock weathering, and eolian deposition. Floods of similar discharge, but with different amounts and characteristics of sediment load, a result of different environmental conditions, led to the observed changes in sediment distributions. A rapid sedimentation predominantly of fines continued until ~30 ka in the Wadis Morikh and Timan (Figure 9).

In unit 3, horizontally adjusted clasts predominate again with evidence of continuous fluvial activity during sedimentation. The portion of the rock fragments from the pavement on top of unit 3 is large (diameter >30 cm). Therefore, the surface must have been affected by flash floods or debris flows for a certain time, or some material was removed. Some time after 30 ka (probably between 19 and 10 ka), the amount of aggrading sediments decreased and incision started. Sedimentation was much lower than earlier and ranges between 0.08 $m yr^{-1}$ in the Wadi Morikh, 0.20 $m yr^{-1}$ in the Khashabi Wadi and 0.30 $m yr^{-1}$ in the Wadi Feiran (Figure 9).

Fine-grained fluvially reworked loess-like eolian sediments similar to unit 2 of profile I in the Wadi Morikh (Figures 4 and 5) have already been described by Rögner *et al.* (1999, 2004), Rögner & Smykatz-Kloss (1998) and Smykatz-Kloss *et al.* (1998, 1999/2000, 2000, 2003) in the middle

reaches of Wadi Feiran. Their earlier interpretation (Rögner *et al.* 1999) of these deposits as lacustrine deposits had to be rejected for most of the investigated sites in Southern Sinai because of the steep gradient of Wadi Feiran. As in the other wadis, no evidence of lacustrine environments could be found (e.g., occurrence of barriers, shoreline, soil horizons, gypsum crystals, mud snails, or settling clays). After re-evaluation of the earlier results, Rögner *et al.* (2004) reinterpreted the interbedded yellowish silty and coarse-grained fluvial sediments. They show chaotic, abrupt, and discontinuous sequences, as deposits of a mixed load river. The river is meandering and transporting coarse-grained material, and during high floods even boulders, as well as fine-grained material in suspension. The composition of the coarse-grained sediments indicates that they are weathering products of the rock outcrops in the wadis. They were deposited at point bars in stream beds, as well as in the former wadi bed by decreasing transport energies or behind massive boulders blocking the flow channels.

The origin of the suspended silty material, deposited as unit 2 in the Wadi Morikh and also found in the Wadi Feiran, is potentially the Gulf of Suez, the bottom of which is a mere 80 m deep. Due to the existence of dolomite within the silts as well as Miocene foraminifera of *Globigerina* sp., Rögner *et al.* (2004) suggest the Ataqa structure (west of the Gulf) to be one of the main sources of the Sinai loess (Crouvi *et al.* 2008; Enzel *et al.* 2008). In the center of the structure Miocene globigerina marls occur (Bayer *et al.* 1988). During the LGM, the global sea level was 120 m lower and the sediments of the desiccated bottom of the Gulf of Suez were exposed (Gvirtzman 1994). The loess-like material was transported to the southwestern Sinai wadis by western to northwestern winds, accumulated on the valley slopes and then reworked and washed by floods back towards the depression which is nowadays the Gulf. According to Rögner *et al.* (2004), during high floods the fine material overtopped the banks of the meandering streams and deposited as overbank fines on the narrow remains of older terraces next to the riverbed. To a smaller extent, the silty material came to these terraces by crevassing of the levees. This explanation also fits the other wadis which provide massive remnants of redeposited eolian sediments. Furthermore, the fluvial transport is indicated by multiple abrupt changes from fine-grained material to coarser sediments. The corresponding climate in the source areas of the wadis in the higher altitudes of the Southern Sinai Mountains (1,000–2,000 m a.s.l.) could have been arid to semi-arid in periods of higher fluvial activity while in the areas below 1,000 m a.s.l., aridity could have persisted.

The youngest fluvial sediments on top of the upper fluvial terrace provide ages of ~19 ka in Wadis Morikh and Eghshy and therefore correlate with the results of Rögner *et al.* (1999), who postulate LGM and post-LGM ages (27–12 ka) for the loess-like reworked sediments in the Wadi Feiran. But the provided OSL ages of the other wadis document an earlier onset of fluvial sediment deposition of about 50 ka. The development of the second fluvial terrace must have taken place around 30 ka (OSL 15, 24, Table 2). The final fluvial accumulations in the Wadi Feiran are much younger (~9 ka). This might be attributed to differences in the fluvial regime and a differing climate because of the higher elevation and greater extension of the Wadi Feiran catchment, which includes the summit area of the Sinai mountains reaching up to more than 2,600 m a.s.l. At this altitude the (hyper) arid climate of today (some 60 mm precipitation yr^{-1} during winter) could have been changed into a semi-arid one with a common snow cover for weeks every year and meltwater floods of different intensity. The OSL ages correlate well with the period of high Lisan Lake levels in the Jordan Valley from 40 to 20 ka (mostly MIS 3) published by Frumkin *et al.* (2011). These indicate a semihumid paleoclimate for the Jordan area. The youngest dates around 10 ka (TL and OSL) of the uppermost (final) fluvial sediments in Wadi Feiran seem, therefore, to be an exception with a close correlation to the winter rain climate of the summit area of Mount Sinai. This was probably characterized by precipitations close to and partly over roughly 100 mm yr^{-1}, a common snow cover and, due to temperatures often ranging below zero a remarkably high frost weathering. The input of clasts by fluvial processes into the upper reaches of Wadi Feiran should have been much higher and lasted longer compared to the other wadis of South Sinai.

The fourth group of sediments is an indicator for abandonment of fluvial terraces and alluvial fans and their incision of the wadi fills. Eolian sediments that cover the fluvial terraces are part of that group and can be used to gain a minimum age of erosion processes within the valleys.

Furthermore, slack-water deposits which remain in rock shelters (e.g., sample OSL 23 in the Wadi Eghshy) and the uppermost parts of massive deposits of the alluvial fans are sediments associated with these wadi incisions. The deposits themselves, however, are evidence of continuing accumulation. There is no evidence that the alluvial fans have approached the Gulf of Suez during the late Quaternary. Today, the wadi fills within the active channels are totally incised back to their respective pre-late Quaternary deposition level; all the way to bedrock. This overall incision must have taken place soon after 19 ka, when fluvial sedimentation ceased in most of the valley aggrading landforms (Figures 6 and 8(a)).

The elevation of the uppermost erosional scarp in the wadis can be correlated with the elevation of the roots of the alluvial fan for each wadi. The fans are currently deeply incised rather than building up. The role of uplift of the Sinai mountains on the observed incision is not yet clear but it was undoubtedly prevented for a long time by the fast rate of aggradation during the late Pleistocene (~50 to ~20 ka).

CONCLUSIONS

The geomorphological and sedimentological results together with the OSL data in the southwestern Sinai wadis indicate their responses to potential climate changes.

1. The absence of sediments >50 ka in the wadis indicates long-term fluvial erosion with only minor exceptions in the southernmost Wadi Khashabi, where eolian sedimentation prevented this effective erosion.
2. Eolian deposits probably affected the southernmost part of the Sinai Peninsula throughout the last 100 ka. During 55–43 ka increased winds are indicated by fossil dunes in the Wadis Morikh and Eghshy. Their subsequent stabilization and fossilization by carbonate-rich water was only possible under reduced wind systems and somewhat wetter conditions after 43 ka. Moderate aridity, but with frequent storm events, as described by Amit *et al.* (2011) in the nearby Negev Desert, are identified as responsible for the accumulation of the thick fluvial deposits from 45 to 35 ka, with special reference to Wadi Morikh. They are characterized by interbeddings of fluvially reworked sediment layers of eolian origin and pure but also fine-grained fluvial material, all distinguishable in three different sediment units.
3. Typical for all wadis is the accumulation of a basal coarse gravel which started around 50 ka and, therefore, prior to the following large wadi fill. Episodic floods and debris flow explain this type of sediment. The fine-grained sediment body is superimposed showing an unconformity at several places. This may indicate a dramatic change to more windy conditions with an increase of sand- and duststorms around 43 ka, but not necessarily a reduction of annual precipitation. The existence of two fluvial, erosion terraces in the wadis are indicative of stronger (episodical) floods at the beginning of an important erosion period younger than 20 ka with a supposedly minor eolian influence. The lower fluvial terrace of several meters height above the valley bottoms has developed obviously later than LGM.
4. Large alluvial fans reflecting the sediment character of the adjacent wadi fills were accumulated at the southwestern Sinai Mountain front. Each alluvial fan is associated with the highest sediment fill in its corresponding wadi. Therefore, the deposition of the fans must have happened synchronously with terrace deposition. Despite large amounts of transported material, the spatial extension of the alluvial fans never reached the shoreline of the Gulf of Suez throughout the late Quaternary. The incision of the fans and the thick wadi fills is the result of a continuous erosion starting around 20 ka (LGM) with the exception of the larger Wadi Feiran. There, the overall incision began at 9 ka which may be explained by the special altitudinal range of the watershed.

ACKNOWLEDGEMENTS

We thank Klaus Heine, Regensburg, for inspiring discussions in the field, as well as Neil Macdonald, Liverpool, and a second anonymous reviewer for their encouragement. Some of the graphics were converted by Thomas Bartsch, Mainz.

REFERENCES

Abdallah, A. & Abu Khadrah, A. 1976 Remarks on the Geomorphology of the Sinai Peninsula and its associated rocks, Egypt. Colloquium on the Geology of the Aegean Region, Athens, Greece, Vol. 1, pp. 509–516.

Amit, R., Enzel, Y. & Sharon, D. 2006 Permanent Quaternary aridity in the southern Negev, Israel. *Geology* **34** (6), 509–512.

Amit, R., Gerson, R. & Yaalon, D. H. 1993 Stages and rate of the gravel shattering process by salts in desert Reg soils. *Geoderma* **57**, 295–324.

Amit, R., Simhai, O., Ayalon, A., Enzel, Y., Matmon, A., Crouvi, O., Porat, N. & McDonald, E. 2011 Transition from arid to hyper-arid environment in the southern Levant deserts as recorded by early Pleistocene cummulic Aridisols. *Quat. Sci. Rev.* **30**, 312–323.

Awad, H. 1951 La Montagne du Sinai Central. Étude Morphologique. *Bulletin de la Societé (Royale) de Géographie*, Le Caire.

Awad, H. 1953 Signification morphologique des depots lacustres de la montagne du Sinai Central. *Bull. Soc. Roy. Géogr.* **25**, 23–28.

Baker, V. R. 1977 Stream-channel response to floods with examples from central Texas. *Geol. Soc. Am. Bull.* **88**, 1057–1071.

Barron, T. 1907 *The Topography and Geology of the Peninsula of Sinai (Western Portion)*. Survey Department, Cairo.

Bayer, H.-J., Hötzl, H., Jade, B., Roscher, B. & Voggenreiter, W. 1988 Sedimentary and structural evolution of the north-west Arabian Red Sea margin. *Tectonophysics* **153**, 137–151.

Bertrams, M., Protze, J., Löhrer, R., Schyle, D., Richter, J., Hilgers, A., Klasen, N., Schmidt, C. & Lehmkuhl, F. 2012 Multiple environmental change at the time of the modern human passage through the Middle East – first results from geoarchaeological investigations on Upper Pleistocene sediments in the Wadi Sabra (Jordan). *Quat. Int.* **274**, 55–72.

Bøtter-Jensen, L., Andersen, C. E., Duller, G. A. T. & Murray, A. S. 2003 Developments in radiation, stimulation and observation facilities in luminescence measurements. *Radiat. Meas.* **37**, 535–541.

Büdel, J. 1954 Sinai, 'die Wüste der Gesetzesbildung' als Beispiel für die allgemeine klimatische Wüstenmorphologie. *Abhandlungen der Akademie für Raumforschung und Landesplanung* **28**, 63–85.

Crouvi, O., Amit, R., Enzel, Y., Porat, N. & Sandler, A. 2008 Sand dunes as a major proximal dust source for late Pleistocene loess in the Negev desert, Israel. *Quat. Res.* **70**, 275–282.

Dayan, U. & Morin, E. 2006 Flash flood producing rainstorms over the Dead Sea: a review. In: *New Frontiers in Dead Sea Paleoenvironmental Research* (Y. Enzel, A. Agnon & M. Stein, eds). Geological Society of America, Boulder, CO, Vol. 401, pp. 53–62.

de Martonne, E. 1947 *Géographie Physique.* 2. Armand Colin, Paris.

Dayan, U., Ziv, B., Margalit, A., Morin, E. & Sharon, D. 2001 A severe autumn storm over the Middle-East: synoptic and mesoscale convection analysis. *Theor. Appl. Climatol.* **69** (1–2), 103–122.

Enzel, Y., Amit, R., Dayan, U., Crouvi, O., Kahana, R., Ziv, B. & Sharon, D. 2008 The climatic and physiographic controls of the eastern Mediterranean over the late Pleistocene climates in the southern Levant and its neighboring deserts. *Glob. Planet. Change* **60**, 165–192.

Fraas, O. 1867 *Aus dem Orient*. Ebner & Seubert, Stuttgart.

Frumkin, A., Bar-Yosef, O. & Schwarcz, H. P. 2011 Possible paleohydrologic and paleoclimatic effects on hominin migration and occupation of the Levantine Middle Paleolithic. *J. Hum. Evol.* **60** (4), 437–451.

Glasby, P., O'Flaherty, A. & Williams, M. A. J. 2010 A geospatial visualization of a late Pleistocene fluvial wetland surface in the Flinders Ranges, South Australia. *Geomorphology* **118**, 130–151.

Graf, W. L. 1988 Definition of flood plains along arid-region rivers. In: *Flood Geomorphology* (V. R. Baker, R. C. Kochel & P. C. Patton, eds). Wiley, New York, pp. 231–242.

Greenbaum, N., Porat, N., Rhodes, E. & Enzel, Y. 2006 Large floods during Late Oxygen Isotope Stage 3, southern Negev desert, Israel. *Quat. Sci. Rev.* **25**, 704–719.

Greenbaum, N., Schick, A. P. & Baker, V. R. 2000 The paleoflood record of a hyperarid catchment, Nahal Zin, Negev Desert, Israel. *Earth Surf. Process. Land.* **25**, 951–971.

Greenwood, N. H. 1997 *The Sinai. A Physical Geography*. University of Texas Press, Austin, TX.

Griffiths, J. 1972 The climate of the United Arabian Republic. *World Surv. Climatol.* **10**, 79–92.

Gvirtzman, D. 1994 Fluctuations of sea level during the past 400,000 years: the record of Sinai, Egypt (northern Red Sea). *Coral Reefs* **13**, 203–214.

Haberlah, D., Williams, M. A. J., Halverson, G., McTainsh, G. H., Hill, S. M., Hrstka, T., Jaime, P., Butcher, A. R. & Glasby, P. 2010a Loess and floods: High-resolution multi-proxy data of Last Glacial Maximum (LGM) slackwater deposition in the Flinders Ranges, semi-arid South Australia. *Quat. Sci. Rev.* **29**, 2673–2693.

Haberlah, D., Glasby, P., Williams, M. A. J., Hill, S. M., Williams, F., Rhodes, E. J., Gostin, V., O'Flaherty, A. & Jacobsen, G. E. 2010b 'Of droughts and flooding rains': an alluvial loess record from central South Australia spanning the last glacial cycle. In: *Australian Landscapes* (P. Bishop & B. Pillans, eds). Geological Society of London, Special Publications 346, London, pp. 185–223.

Har-El, M. 1983 *Sinai Journeys. The Route of the Exodus*. Ridgefield Publishing Co, San Diego, CA.

Heine, K. & Völkel, J. 2009 Desert flash flood series. Slack water deposits and floodouts in Namibia: their significance for paleoclimatic reconstructions. *Zbl. Geol. Paläont.* **I** (3–4), 287–308.

Heine, K. & Völkel, J. 2010 Soil clay minerals in Namibia and their significance for the terrestrial and marine past global change research. In: *Quaternary and Environmental Geomorphology* (K. Mizuno, ed). African Study Monographs, Center for

African Area Studies, Kyoto University, Kyoto, Japan, Suppl. 40, pp. 31–50.

Heine, K. & Völkel, J. 2011 Extreme floods around AD 1700 in the southern Namib Desert, Namibia, and in the Orange River catchment, South Africa. Were they forced by a decrease of solar irradiation during the Little Ice Age? *Geogr. Polonica* **84**, 61–80.

Hürkamp, K., Raab, T. & Völkel, J. 2009 Two and three-dimensional quantification of lead contamination in alluvial soils of a historic mining area using field portable X-ray fluorescence (FPXRF) analysis. *Geomorphology* **110** (1–2), 28–36.

Imbrie, J., Hays, J. D., Martinson, D. G., McIntyre, A., Mix, A. C., Morley, J. J., Pisias, N. G., Prell, W. L. & Shackleton, N. J. 1984 The orbital theory of Pleistocene climate: support from revised chronology of marine $\delta^{18}O$ record. In: *Milankovitch and Climate. Part 1* (A. L. Berger, J. Imbrie, J. Hays, G. Kukla & B. Saltzman, eds). Springer, Dordrecht, pp. 269–305.

Issar, A. & Eckstein, Y. 1969 The lacustrine beds of Wadi Firan, Sinai: their origin and significance. *Israel J. Earth Sci.* **18**, 21–27.

Jain, M., Murray, A. S. & Bøtter-Jensen, L. 2003 Characterisation of blue-light stimulated luminescence components in different quartz samples: implications for dose measurement. *Radiat. Meas.* **37**, 441–449.

Kahana, R., Ziv, B., Enzel, Y. & Dayan, U. 2002 Synoptic climatology of major floods in the Negev Desert, Israel. *Int. J. Climatol.* **22**, 867–882.

Kehew, A. E., Milewski, A. & Soliman, F. 2010 Reconstructing an extreme flood from boulder transport and rainfall-runoff modelling: Wadi Isla, South Sinai, Egypt. *Glob. Planet. Change* **70**, 64–75.

Klaer, W. 1962 Die periglaziale Höhenstufe in den Gebirgen Vorderasiens. Ein Beitrag zur Morphogenese der Hochgebirge in den subtropischen Breiten. *Z. Geomorphol. N.F.* **6**, 17–32.

Knabe, K. 2000 *Sedimentpetrographische und geochemische Untersuchungen an Sedimenten im Wadi Feiran (Südsinai) zur Klärung ihrer Herkunft und Ablagerungsbedingungen – Paläoklimatische Überlegungen.* Dissertation, Universität Karlsruhe, Germany.

Leopold, M., Völkel, J. & Heine, K. 2006 A ground-penetrating radar survey of late Holocene fluvial sediments in NW Namibian river valleys: characterization and comparison. *J. Geol. Soc.* **163**, 923–936.

Mix, A. C., Bard, E. & Schneider, R. 2001 Environmental processes of the ice age: land, oceans, glaciers (EPILOG). *Quat. Sci. Rev.* **20**, 627–657.

Murray, A. S. & Wintle, A. G. 2000 Luminescence dating of quartz using an improved single-aliquot regenerative-dose protocol. *Radiat. Meas.* **32**, 57–73.

Murray, A. S. & Wintle, A. G. 2003 The single aliquot regenerative dose protocol: potential for improvements in reliability. *Radiat. Meas.* **37**, 377–381.

Murray, A. S., Marten, R., Johnston, A. & Martin, P. 1987 Analysis for naturally occurring radionuclides at environmental concentrations by gamma spectrometry. *J. Radioanal. Nucl. Chem.* **115**, 263–288.

Nir, D. 1970 Les lacs quaternaires dans la region de Feiran, Sinai Central. *Rév. Géogr. Phys. Géol.* **12**, 335–346.

Nir, D. 1974 Lacustrine/fluviatile sediments in Firan and Tarfat el Kudrein. *Z. Geomorphol. N.F. Suppl.* **22**, 32–34.

Olley, J. M., Murray, A. S. & Roberts, R. G. 1996 The effects of disequilibria in the uranium and thorium decay chains on burial dose rates in fluvial sediments. *Quat. Sci. Rev.* **15**, 751–760.

Prescott, J. R. & Hutton, J. T. 1994 Cosmic ray distributions to dose rates for luminescence and ESR dating: large depths and long-term variations. *Radiat. Meas.* **23**, 497–500.

Rögner, K. & Smykatz-Kloss, W. 1998 The fine-grained, loess-like sediments of the Wadi Firan, Sinai, Egypt: possibilities of palaeoclimatic interpretations? In: *Quaternary Deserts and Climatic Change* (A. S. Alsharhan, K. W. Glennie, G. L. Whittle & C. G. S. C. Kendall, eds). Balkema, Rotterdam, pp. 209–211.

Rögner, K., Knabe, K., Roscher, B., Smykatz-Kloss, W. & Zöller, L. 2004 Alluvial loess in the Central Sinai: occurrence, origin, and palaeoclimatological consideration. *Lect. Notes Earth Sci.* **102**, 79–99.

Rögner, K., Smykatz-Kloss, W. & Zöller, L. 1999 Oberpleistozäne paläoklimatische Veränderungen im Zentral-Sinai (Ägypten). *Erdkunde* **53**, 220–230.

Sherief, Y. S. Y. 2008 *Flash Floods and their Effects on the Development in El-Qaa Plain Area in South Sinai, Egypt, a Study in Applied Geomorphology using GIS and Remote Sensing.* Dissertation, Johannes-Gutenberg-Universität Mainz, Germany.

Singarayer, J. S. & Bailey, R. M. 2003 Further investigations of the quartz optically stimulated luminescence components using linear modulation. *Radiat. Meas.* **37**, 451–458.

Smykatz-Kloss, W., Knabe, K., Rögner, K. & Hüttl, C. 1998 Paleoclimatic changes in central Sinai. *Palaeoecol. Afr.* **25**, 143–155.

Smykatz-Kloss, W., Roscher, B., Knabe, K., Rögner, K. & Zöller, L. 1999/2000 Wüstenforschung und Paläoklimatologie im zentralen Sinai. *Chemie Erde* **59**, 245–258.

Smykatz-Kloss, W., Roscher, B. & Rögner, K. 2000 Gab es im Sinai pleistozäne Seen? *Regensburger Geographische Schriften* **33**, 127–139.

Smykatz-Kloss, W., Roscher, B. & Rögner, K. 2003 Pleistocene lakes in central Sinai, Egypt. In: *Desertification in the Third Millennium* (A. S. Alsharhan, K. W. Glennie, W. W. Wood, A. S. Goudie, A. Fowler & E. M. Abdellatif, eds). Swets & Zeitlinger Publishers, Lisse, The Netherlands, pp. 111–116.

Tooth, S. 2000 Process, form and change in dryland rivers: a review of recent research. *Earth Sci. Rev.* **51**, 67–107.

Völkel, J. 1995 *Periglaziale Deckschichten und Böden im Bayerischen Wald und seinen Randgebieten als geogene Grundlagen landschaftsökologischer Forschung im Bereich naturnaher Waldstandorte*. Zeitschrift für Geomorphologie N.F. Suppl. 96. Bornträger, Berlin.

First received 11 November 2011; accepted in revised form 6 July 2012. Available online 5 December 2012